Available online at www.sciencedirect.com
SCIENCE DIRECT®
Journal of Organometallic Chemistry 690 (2005) 4001–4017
Journal of Organometallic Chemistry
www.elsevier.com/locate/jorganchem

Chalcogen-capped ruthenium carbonyl clusters derived from diphosphazane mono- and dichalcogenides of the type $X_2P(E)N(R)PX_2$ and $X_2P(E)N(R)P(E)X_2$ (E = S or Se) ☆

Thengarai S. Venkatakrishnan, Setharampattu S. Krishnamurthy *,[1], Munirathinam Nethaji

Department of Inorganic and Physical Chemistry, Indian Institute of Science, Bangalore 560012, India

Received 4 March 2005; accepted 6 May 2005
Available online 14 July 2005

Abstract

Reactions of $Ru_3(CO)_{12}$ with diphosphazane monoselenides $Ph_2PN(R)P(Se)Ph_2$ [R = (*S*)-*CHMePh (**L**^{4}), R = $CHMe_2$ (**L**^{5})] yield mainly the selenium bicapped tetraruthenium clusters $[Ru_4(\mu_4\text{-}Se)_2(\mu\text{-}CO)(CO)_8\{\mu\text{-}P,P\text{-}Ph_2PN(R)PPh_2\}]$ (**1**, **3**). The selenium monocapped triruthenium cluster $[Ru_3(\mu_3\text{-}Se)(\mu_{sb}\text{-}CO)(CO)_7\{\kappa^2\text{-}P,P\text{-}Ph_2PN((S)\text{-}*CHMePh)PPh_2\}]$ (**2**) is obtained only in the case of **L**^{4}. An analogous reaction of the diphosphazane monosulfide $(PhO)_2PN(Me)P(S)(OPh)_2$ (**L**^{6}) that bears a strong π-acceptor phosphorus shows a different reactivity pattern to yield the triruthenium clusters, $[Ru_3(\mu_3\text{-}S)(\mu_3\text{-}CO)(CO)_7\{\mu\text{-}P,P\text{-}(PhO)_2PN(Me)P(OPh)_2\}]$ (**9**) (single sulfur transfer product) and $[Ru_3(\mu_3\text{-}S)_2(CO)_5\{\kappa^2\text{-}P,P\text{-}(PhO)_2PN(Me)P(OPh)_2\}\{\mu\text{-}P,P\text{-}(PhO)_2PN(Me)P(OPh)_2\}]$ (**10**) (double sulfur transfer product). The reactions of diphosphazane dichalcogenides with $Ru_3(CO)_{12}$ yield the chalcogen bicapped tetraruthenium clusters $[Ru_4(\mu_4\text{-}E)_2(\mu\text{-}CO)(CO)_8\{\mu\text{-}P,P\text{-}Ph_2PN(R)PPh_2\}]$ [R = (*S*)-*CHMePh, E = S (**6**); R = $CHMe_2$, E = S (**7**); R = $CHMe_2$, E = Se (**3**)]. Such a tetraruthenium cluster $[Ru_4(\mu_4\text{-}S)_2(\mu\text{-}CO)(CO)_8\{\mu\text{-}P,P\text{-}(PhO)_2PN(Me)P(OPh)_2\}]$ (**11**) is also obtained in small quantities during crystallization of cluster **9**. The dynamic behavior of cluster **10** in solution is probed by NMR studies. The structural data for clusters **7**, **9**, **10** and **11** are compared and discussed.

Keywords: Ruthenium; Cluster compounds; P ligands; Chalcogen clusters; Cluster dynamics; X-ray crystallography

1. Introduction

Chalcogen bridged transition metal clusters bearing mono- and bidentate phosphorus ligands [1–3] have been the subject of several recent publications. In such clusters, the chalcogen element plays an important role in stabilizing the bonding network. Furthermore, these clusters have the ability to add or remove ligands or electrons while still retaining their integrity. Such chalcogen bridged clusters can be regarded as models for extended inorganic solids [4] and have been utilized for cluster growth reactions [5] and synthesis of heterometallic clusters [6]. Chalcogen bridged clusters bearing phosphorus ligands are synthesized by one of the following routes: (1) treatment of a zero-valent metal carbonyl of the type $M_3(CO)_{12}$ (M = Fe, Ru, Os) with a phosphine chalcogenide $R_3P(E)$ (E = S, Se) in the presence of Me_3NO as a decarbonylating agent [7], (2) reaction of a chalcogen-bridged cluster with a phosphine [8], (3) reaction of a phosphine substituted cluster with H_2S [9a] and (4) reaction of phosphine

☆ Part 23 of the series "Organometallic chemistry of diphosphazanes"; for Part 22, see [19e].

* Corresponding author. Tel.: +91 80 22932401; fax: +91 80 23600683/23601552.
E-mail address: sskrish@ipc.iisc.ernet.in (S.S. Krishnamurthy).
[1] INSA Senior Scientist.

0022-328X/$ - see front matter © 2005 Elsevier B.V. All rights reserved.
doi:10.1016/j.jorganchem.2005.05.041

substituted hydrido cluster with elemental chalcogen [9b]. The first route takes advantage of the reactivity of the P=E bond to undergo oxidative addition across the M_3 core thereby transferring the chalcogen to the transition metal with concomitant coordination of the phosphine ligand. In the case of bidentate ligands, the ligand can coordinate either in a chelating or bridging fashion depending on the reaction conditions, the bite angle of the diphosphine and the transition metal employed.

Chalcogen(E) bridged carbonyl clusters bearing monophosphines of the type PR_3 (R = Ph [7,8b,8e, 10], *p*-tolyl [10a], C_6H_4 (OMe-4) [10b] or C_6H_2\{$(OMe)_3$-2,4,6\} [11]) and PR_2R' (R = Me, R′ = Ph [8a]; R = Ph, R′ = benzyl [10b], Me [5], OMe [5], 2-thienyl [12a], (2-pyridyl)-2-thienyl [12b] or 2-pyridyl [12c]) have been investigated to obtain both tri- and tetranuclear clusters of different structural types. Extensive studies have also been reported on a variety of chalcogen bridged carbonyl clusters bearing diphosphines of the type $(Ph_2P)_2R$ (R = C≡C, E = Se, M = Ru [8d]; R = CH_2, E = S, M = Os [9a]; R = CH_2, E = Se, M = Fe [13a], Ru [8e,13b,13c], Os [9b]; R = CH_2, E = Te, M = Ru [8b]; R = $(CH_2)_2$, E = Se, M = Fe [13a], Ru [8e,13d]; R = $(CH_2)_3$, E = Se, M = Ru [8c]; R = $(C_5H_4)_2$ Fe, E = Se, M = Fe [13a], Ru [13d,13e]; R = C_6H_4\{$(CH_2)_2$-1,2)\}, E = S, M = Ru [11]; R = C_6H_4 $(CH_2)_2$-1,2), E = Se, M = Fe, Ru [14]; R = $C_5H_2O_2$, E = S, M = Ru [15]). Chalcogen bridged heterometallic clusters bearing both mono- and diphosphines have been reported recently by Predieri [5] and Braunstein [16]. On the other hand, there are only two reports [17] on the analogous chalcogen bridged clusters bearing diphosphazanes as ancillary ligands. Woollins and co-workers studied the reactivity of diphosphazane dichalcogenides $R_2P(E)N(H)P(E)R_2$ (R = Ph, E = S or Se; R = ^{i}Pr, E = S) towards $Ru_3(CO)_{12}$ to obtain the *closo* clusters $[Ru_4(\mu_4\text{-}E)_2(\mu\text{-}CO)(CO)_8\{\mu\text{-}P,P\text{-}R_2PN(H)PR_2\}]$ as the main products. In these clusters, the diphosphazane $R_2PN(H)PR_2$ adopts a bridging mode of co-ordination [17a]. Raghuraman et al. reported the reactivity of diphosphazane monosulfides $Ph_2P(S)N(R)PPh_2$ (R = (*S*)-*CH-MePh or $CHMe_2$) towards $Ru_3(CO)_{12}$ and isolated sulfur-monocapped clusters, $[Ru_3(\mu_3\text{-}S)(\mu_{sb}\text{-}CO)(CO)_7\{\kappa^2\text{-}P,P\text{-}Ph_2PN(R)\text{-}PPh_2\}]$ in which the diphosphazane adopts a chelating mode of coordination [17b]. Recently we have studied the radical initiated substitution of CO in $Ru_3(CO)_{12}$ by axially chiral diphosphazanes in which the diphosphazane adopts a bridging mode of coordination [18]. As a part of our research program [17b–19] on the organometallic chemistry of "P–N–P" type ligands [20], we report here the results of our investigations on the reactions of chiral and achiral diphosphazane mono- and dichalcogenides with $Ru_3(CO)_{12}$.

2. Experimental

2.1. General

All reactions and manipulations were carried out under an atmosphere of dry nitrogen using standard Schlenk and vacuum-line techniques. The solvents were purified by standard procedures and distilled under nitrogen prior to use. The NMR spectra (^{1}H, ^{13}C\{^{1}H\} and ^{31}P\{^{1}H\}) were recorded in $CDCl_3$ at 298 K using Bruker ACF-200, Bruker AMX-400 or Bruker Avance-400 spectrometers. Two-dimensional ^{31}P–^{31}P COSY, ^{31}P–^{31}P phase sensitive NOESY, ^{1}H–^{1}H ROESY and ^{31}P–^{1}H COSY spectra were recorded either on a Bruker AMX-400 MHz or Bruker Avance-400 MHz spectrometer using standard pulse sequences. IR spectra were recorded using a Bruker FT-IR spectrometer; for this purpose, the sample was spread as a thin film on a KBr disk. Elemental analyses were carried out using a Perkin–Elmer 2400 CHN analyser. Melting points were recorded in a Buchi B-540 melting point apparatus and were uncorrected. The diphosphazane ligands $X_2PN(R)PX_2$ (X = Ph, R = (*S*)-*CHMePh (**L^1**) [21a], $CHMe_2$ (**L^2**) [21b]; R = Me, X = OPh (**L^3**) [21c,21d]) and the chalcogenides $Ph_2PN((S)\text{-}*CHMePh)P(Se)Ph_2$ (**L^4**) [22] and $Ph_2P(S)\text{-}N((S)\text{-}*CHMePh)P(S)Ph_2$ (**L^7**) [23] were prepared by previously reported procedures. Me_3NO (Aldrich), C_6D_6 (Aldrich), $Ru_3(CO)_{12}$ (Strem chemicals) were used as received.

2.1.1. Synthesis of $Ph_2P(Se)N(CHMe_2)PPh_2$ (**L^5**)

The title compound was prepared by following the same procedure as that for **L^4**. Elemental selenium (0.056 g, 0.705 mmol) was added to a solution of $Ph_2PN(CHMe_2)PPh_2$ (0.301 g, 0.705 mmol) in THF (10 cm^3). The reaction mixture was stirred at 25 °C for 18 h and solvent was evaporated to obtain an oil. Methanol (5–10 cm^3) was added to precipitate the title compound. Yield: 42%. M.p. 124–125 °C. Anal. Calc. for $C_{27}H_{27}NP_2Se$: C, 64.0; H, 5.3; N, 2.8. Found: C, 64.0; H, 5.3; N, 1.8%.

2.1.2. Synthesis of $(PhO)_2P(S)N(Me)P(OPh)_2$ (**L^6**)

A mixture of $(PhO)_2PN(Me)P(OPh)_2$ (1.000 g, 2.16 mmol) and elemental sulfur (0.069 g, 2.16 mmol) was dissolved in acetonitrile (35 cm^3) and the mixture heated under reflux for 10 h. Evaporation of solvent from the reaction mixture resulted in an oil. The oil was dissolved in hot methanol and kept at 0 °C overnight to obtain a colorless air-sensitive solid of **L^6**. Yield: 70%. M.p. 132–133 °C. Anal. Calc. for $C_{25}H_{23}NO_4P_2S$: C, 60.5; H, 4.6; N, 2.8; S, 6.5. Found: C, 60.5; H, 4.6; N, 2.9; S, 6.4%. The analogous disulfide was synthesized by the reaction of **L^6** with elemental sulfur but attempts to obtain the compound in a pure form were unsuccessful. The NMR spectroscopic data for the

disulfide were as follows. ^{1}H NMR ($CDCl_3$, 400 MHz): 7.4–7.2 (m, aryl protons), 3.59(t, ^3J(P,H) = 12 Hz, *Me*, N–Me). $^{31}P\{^1H\}$ NMR ($CDCl_3$, 162 MHz): 61.6(s).

2.1.3. Synthesis of $Ph_2P(S)N((S)$-*$CHMePh)P(S)Ph_2$ (L^7)

The title compound $\mathbf{L^7}$ was prepared by following the literature procedure. However, in addition to $\mathbf{L^7}$, the reaction also gave another known dichalcogenide $Ph_2P(S)N(H)P(S)Ph_2$ as described below.

A mixture of $\mathbf{L^1}$ (0.200 g, 0.41 mmol) and elemental sulfur (0.026 g, 0.82 mmol) was heated under reflux in THF (10 cm^3) for 8 h. Solvent was evaporated to dryness and the resulting oil was subjected to column chromatography (a column of dimensions 20×1.5 cm was used) using benzene–petroleum ether (b.p. 60–80 °C) (35:65 v/v) as eluant. Evaporation of the solvent from the first fractions gave the title compound as a colorless solid. Yield: 30%. M.p. 123–125 °C. Further elution followed by evaporation of the eluant afforded a solid which displayed a singlet at 57.2 ppm in its ^{31}P NMR spectrum. The ^{1}H NMR spectrum of this compound showed a singlet at 4.38 ppm (1H) and a multiplet at 7.9–7.3 ppm (20H). Colorless single crystals of the product were obtained by slow evaporation of its benzene solution. Preliminary X-ray crystallographic study gave the cell parameters which were close to those reported for $Ph_2P(S)N(H)P(S)Ph_2$ [24]. Attempts to obtain the title compound exclusively by the reaction of $Ph_2PN((S)$-*$CHMePh)P(S)Ph_2$ [17b] with elemental sulfur also resulted in the same mixture of products.

2.1.4. Synthesis of $Ph_2P(E)N(CHMe_2)P(E)Ph_2$ [E = S (L^8), Se (L^9)]

A mixture of $Ph_2PN(CHMe_2)PPh_2$ (1.000 g, 2.34 mmol) and two equivalents of chalcogen (0.150 g, for E = S, 0.370 g for E = Se, 4.68 mmol) in benzene (35 cm^3) was heated under reflux at 80 °C for 1 day. Evaporation of solvent resulted in an oil. The oil was dissolved in hot methanol and the solution kept at 0 °C to give the diphosphazane dichalcogenides as colorless solids. E = S ($\mathbf{L^8}$): Yield: 25%. M.p. 189–190 °C. Anal. Calc. for $C_{27}H_{27}NP_2S_2$: C, 66.0; H, 5.5; N, 2.9. Found: C, 65.9; H, 5.3; N, 3.3%. E = Se ($\mathbf{L^9}$): Yield: 36%. M.p. 188–190 °C. Anal. Calc. for $C_{27}H_{27}NP_2Se_2$: C, 55.4; H, 4.6; N, 2.4. Found: C, 54.9; H, 4.3; N, 1.8%.

The spectroscopic data for the diphosphazane chalcogenides $\mathbf{L^4}$–$\mathbf{L^9}$ are presented in Table 1.

2.1.5. General procedure for the synthesis of clusters 1–11

In a typical reaction, a 50 cm^3 double-necked round bottom flask was charged with $Ru_3(CO)_{12}$ (0.050 g, 0.078 mmol) and diphosphazane mono- or dichalcogenide (0.078 mmol) under nitrogen. The mixture was dissolved in toluene (20 cm^3). Me_3NO (0.006 g, 0.009 mmol, 1.1 eq.) was added and the solution heated under reflux for 1.5 h (in the case of diphosphazane dichalcogenides, the reaction employed 2.2 molar equivalents of Me_3NO and the reaction time was 2.5 h). At the end of the reaction, solvent was evaporated from reaction mixture and the residue dissolved in dichloromethane (2 cm^3) and subjected to preparative scale thin-layer chromatography over silica-gel using dichloromethane–petroleum ether (b.p. 60–80 °C) (1:1 v/v) as eluant. The eluted bands were separated and the product was extracted into dichloromethane. The dichloromethane solvent was evaporated and the residue crystallised from dichloromethane solution layered with petroleum ether. The infrared spectroscopic and NMR (^{1}H, ^{31}P) data for the ruthenium carbonyl clusters are presented in Table 2. The remaining data are listed below.

2.1.6. $[Ru_4(\mu_4\text{-}Se)_2(\mu\text{-}CO)(CO)_8\{\mu\text{-}P,P\text{-}Ph_2PN((S)$-*$CHMePh)PPh_2\}]$ (1)

The reaction of $Ru_3(CO)_{12}$ with $\mathbf{L^4}$ mainly gave the tetraruthenium cluster **1** (R_f = 0.70) and the triruthenium

Table 1
^{1}H and ^{31}P NMR[a] data for the ligands $\mathbf{L^4}$–$\mathbf{L^9}$

	$^{31}P\{^1H\}$		$^2J_{A\text{-}X}$(Hz)	$\Delta\delta$[b]		^{1}H	
	P_A	P_X		P_A	P_X	C*H*[c]	CH_3[d]
$\mathbf{L^4}$	68.5(d)[e,f]	51.3(s, br)[g]	7.0	+16.3	−0.9	5.30	1.85
$\mathbf{L^5}$	64.3(d)[e,h]	54.3(d)[g]	50.8	+15.5	+5.5	4.07	1.24
$\mathbf{L^6}$	60.0(d)[e]	132.5(d)[g]	102.1	−3.0	−75.5	–	3.26[i]
$\mathbf{L^7}$	69.8(s, br)[e]	–	–	+17.6	–	5.30	1.73
$\mathbf{L^8}$	67.2(s, br)[e]	–	–	+18.4	–	4.13	1.26
$\mathbf{L^9}$	68.0(s, br)[e]	–	–	+19.2	–	4.21	1.28

[a] Recorded in $CDCl_3$.
[b] $\Delta\delta = \delta_{P(\text{chalcogenide derivative})} - \delta_{P(\text{parent diphosphazane})}$.
[c] C*H*-protons of the CHMePh or $CHMe_2$ appear as multiplets.
[d] CH_3 protons of the CHMePh or $CHMe_2$ are doublets with ^3J(H,H) = 7.0 Hz.
[e] P(V) phosphorus.
[f] J(P–Se) = 759.5 Hz.
[g] P(III) phosphorus.
[h] J(P–Se) = 750.0 Hz.
[i] Recorded in C_6D_6 (200 MHz), N–CH_3 (dd, ^3J(P,H) = 11.3, 1.7 Hz).

Table 2
NMR[a] (^{1}H and ^{31}P) and IR data for the ruthenium carbonyl clusters synthesised in the present study

	$^{31}P\{^1H\}$	$\Delta\delta$[b]	^1H		IR (ν_{CO} cm^{-1})
			C*H*[c]	C*H*$_3$[d]	
1	82.8(s)	+30.6[e]	4.95(m)	1.02(d, br)	2043(m), 2005(s), 1959(m, br), 1854(w), 1809(m, br, μ-CO)
2	65.6(s)	+13.4[e]	4.55(m)	1.24(d)	2056(m), 2044(sh), 2014(s), 1984(m), 1946(sh), 1874(w)
3	82.5(s)	+33.7[f]	3.93(m)	0.48(d)	2059(m), 2040(m), 2002(s), 1961(w), 1809(w, br, μ-CO)
4a	86.2(s)	+37.4[f]	3.76(m)[g]	0.36(d)	2078(sh), 2061(m), 2043(w), 2027(sh), 1990(w, br)[g]
4b	95.3,84.2 (d, ^2J(P,P) = 52.8 Hz)	+46.5, 35.4[f]	–	0.82(d)	–
6	85.2(s)	+33.0[e]	4.95(m)	1.28(d)	2046(m), 2009(s), 1965(m), 1813(m, br)
7	81.2(s)	+32.4[f]	3.95(m)	0.38(d)	2060(m), 2040(m), 2003(s), 1961(w), 1809(w, br, μ-CO)
8	94.4, 84.6 (d, ^2J(P,P) = 56.4 Hz)	+45.6, +35.8[e]	4.20(m)	1.23, 0.38(d)	2065(s), 2030(m), 1991(s)
9	143.8(s)	+8.3[h]	–	3.11(t)[i]	2080(m), 2033(m), 2007(w, sh), 1821(w), 1701(m, μ_3-CO)
10	[j]	–	–	3.23 (t),[k] 2.88 (br),[l] 2.47 (t)[m]	2079(w), 2057(w) 2037(w, sh), 2020(w), 1997(m), 1951(w, br)

[a] Recorded in $CDCl_3$.
[b] $\Delta\delta = \delta$(complex) – δ(free diphosphazane).
[c] C*H*-protons of the CHMePh or $CHMe_2$ appear as multiplets.
[d] C*H*$_3$ protons of the CHMePh or $CHMe_2$ are doublets with ^3J(H,H) = 7.0 Hz.
[e] Free ligand is **L^1**.
[f] Free ligand is **L^2**.
[g] **4a** + **4b**.
[h] Free ligand is **L^3**.
[i] ^3J(P,H) = 7.0 Hz.
[j] Exists as two isomers **10** and **10a**; see Fig. 6 for assignment of resonances.
[k] ^3J(P,H) = 7.0 Hz, N–C*H*$_3$, bridging diphosphazane of **10** and **10a**.
[l] N–C*H*$_3$, chelating diphosphazane of **10**.
[m] ^3J (P,H) = 10.0 Hz, N–C*H*$_3$, chelating diphosphazane of **10a**.

cluster **2** (R_f = 0.90) as the isolable products of which **1** is the major product. Analytical data for **1**: Yield: 20%. M.p. 172–173 °C (dec). Anal. Calc. for $C_{41}H_{29}NO_9P_2Se_2Ru_4$: C, 37.7; H, 2.2; N, 1.1. Found: C, 38.1; H, 2.2; N, 0.9%. $^{13}C\{^1H\}$ NMR ($CDCl_3$, 100 MHz): 202.9(br, *C*O, Ru–CO), 197.6(s, *C*O, Ru–CO), 66.2(s, *C*H, CHMePh), 22.4(s, *Me*, CHMePh).

2.1.7. [Ru$_4$(μ$_4$-Se)$_2$(μ-CO)(CO)$_8${μ-P,P-Ph$_2$PN-(CHMe$_2$)PPh$_2$}] (3)

The reaction of $Ru_3(CO)_{12}$ with **L^5** gave a mixture of several products from which the tetraruthenium cluster **3** (R_f = 0.70) and the triruthenium cluster **4** (R_f = 0.80) were isolated and characterised. Analytical data for **3**: Yield: 30%. M.p. 181–183 °C (dec). Anal. Calc. for $C_{37}H_{29}NO_9P_2Se_2Ru_4Cl_2$: C, 33.5; H, 2.2; N, 1.1. Found: C, 33.0; H, 2.5; N, 1.7%. $^{13}C\{^1H\}$ NMR ($CDCl_3$, 100 MHz): 199.0(br, *C*O, Ru–CO), 197.2(br, *C*O, Ru–CO), 61.3(t, ^2J(P,C) = 4.6 Hz, *C*H, $CHMe_2$), 23.9(s, *Me*, $CHMe_2$). Another compound **5** with an R_f value of 0.90 was also isolated from the reaction mixture which was tentatively formulated as a diruthenium species bearing a bridging diphosphazane. The spectroscopic data for compound **5** are as follows. IR (neat, ν_{CO} cm^{-1}): 2053(s), 2039(w), 2011(m), 1999(m), 1986(m). ^{1}H NMR ($CDCl_3$, 400 MHz): 7.8–7.4 (m, aryl protons), 3.50 (m, C*H*, $CHMe_2$), 0.48 (d, ^3J(H,H) = 7.0 Hz, *Me*, $CHMe_2$). $^{31}P\{^1H\}$ NMR ($CDCl_3$, 162 MHz): 82.5(s).

2.1.8. [Ru$_4$(μ$_4$-S)$_2$(μ-CO)(CO)$_8${μ-P,P-Ph$_2$PN((S)-*CHMePh)PPh$_2$}] (6)

The reaction of $Ru_3(CO)_{12}$ with **L^7** gave the tetraruthenium cluster **6** (R_f = 0.70) as the only isolable product. Yield: 13%. M.p. 179–181 °C (dec). Anal. Calc. for $C_{41}H_{29}NO_9P_2S_2Ru_4$: C, 40.7; H, 2.4; N, 1.2. Found: C, 40.0; H, 2.3; N, 1.0%.

2.1.9. [Ru$_4$(μ$_4$-S)$_2$(μ-CO)(CO)$_8${μ-P,P-Ph$_2$PN-(CHMe$_2$)PPh$_2$}] (7)

The reaction of $Ru_3(CO)_{12}$ with **L^8** gave the tetraruthenium cluster **7** (R_f = 0.70) and the triruthenium cluster **8** (R_f = 0.80). Analytical data for **7**: Yield: 28%. M.p. 188–190 °C (dec). Anal. Calc. for $C_{37}H_{29}NO_9P_2S_2Ru_4Cl_2$: C, 36.0; H, 2.4; N, 1.1. Found: C, 35.8; H, 2.0; N, 0.6%.

2.1.10. [Ru$_3$(μ$_3$-S)(μ$_3$-CO)(CO)$_7${μ-P,P-(PhO)$_2$-PN(Me)P(OPh)$_2$}] (9) and [Ru$_3$(μ$_3$-S)$_2$(CO)$_5$-{μ-P,P-(PhO)$_2$PN(Me)P(OPh)$_2$}{κ^2-P,P-(PhO)$_2$-PN(Me)P(OPh)$_2$}] (10)

The reaction of $Ru_3(CO)_{12}$ with **L^6** gave the triruthenium clusters **9** (R_f = 0.90) and **10** (R_f = 0.70) as the isolable products. Even when the reaction was carried out in the presence of 2 equivalents of **L^6**, both the clusters **9** and **10** were obtained and isolated. Cluster **10** was also formed in the reaction of **9** with **L^6** in boiling toluene in the presence of Me_3NO and could be isolated from the

reaction mixture by PTLC. Analytical data for **9**: Yield: 45%. M.p. 181–183 °C (dec). Anal. Calc. for $C_{33}H_{23}NO_{12}P_2SRu_3$: C, 38.7; H, 2.2; N, 1.4; S, 3.1. Found: C, 37.5; H, 2.7; N, 1.5; S, 3.1%. $^{13}C\{^1H\}$ NMR ($CDCl_3$, 100 MHz): 199.1(s, *C*O, Ru–CO), 194.9(s br, *C*O, Ru–CO), 30.8(t, ^2J(P,C) = 3.7 Hz, *Me*, N–Me). Analytical data for **10**: Yield: 9%. M.p. 201–205 °C (dec). Anal. Calc. for $C_{55}H_{46}N_2O_{13}P_4S_2Ru_3$: C, 46.0; H, 3.2; N, 2.0. Found: C, 45.8; H, 2.9; N, 1.5%. $^{13}C\{^1H\}$ NMR ($CDCl_3$, 100 MHz): 199.2(d, ^2J(P,C) = 11.0 Hz, *C*O, Ru–CO, adjacent to bridging diphosphazane), 198.5(m br, *C*O, Ru–CO), 196.7(m br, *C*O, Ru–CO), 195.1(br, *C*O, Ru–CO), 192.9(t, ^2J(P,C) = 12.9 Hz, *C*O, Ru–CO, adjacent to chelating diphosphazane), 30.4(br, *Me*, N–Me), 30.3(t, ^2J(P,C) = 3.7 Hz, *Me*, N–Me), 29.8(br, *Me*, N–Me), 29.5(br, *Me*, N–Me).

2.1.11. Reaction of $[Ru_3(\mu_3\text{-}S)(\mu_{sb}\text{-}CO)(CO)_7\{\kappa^2\text{-}P,P\text{-}Ph_2PN((S)\text{-}*CHMePh)PPh_2\}]$ (*A*) with $(PhO)_2PN(Me)P(S)(OPh)_2$ (**L⁶**)

The ruthenium cluster **A** was prepared as reported previously [17b]. A mixture of $Ru_3(CO)_{12}$ (0.050 g, 7.82×10^{-5} mol) and diphosphazane monosulfide $Ph_2PN((S)\text{-}*CHMePh)P(S)Ph_2$ (0.041 g, 7.82×10^{-5} mol) was dissolved in toluene (20 cm^3). Me_3NO (0.006 g, 9.00×10^{-5} mol) was added and the reaction mixture was heated to 105 °C for 1 h. The reaction mixture was cooled to ambient temperature and the solvent evaporated to dryness. The dark red residue which consisted essentially of **A** (^{31}P NMR evidence) was dissolved in toluene (20 cm^3); **L⁶** (0.039 g, 7.82×10^{-5} mol) and Me_3NO (0.006 g, 9.00×10^{-5} mol) were added and the mixture was heated under reflux for 1 h. Solvent was evaporated; the residue was dissolved in dichloromethane (2 cm^3) and subjected to preparative scale thin-layer chromatography [dichloromethane-petroleum ether (b.p. 60–80 °C) (1:1 v/v) as eluant] to isolate a solid sample for which the following spectroscopic data were obtained.

IR (neat, ν_{CO} cm^{-1}): 2036(s), 1982(s). ^1H NMR ($CDCl_3$, 400 MHz): 7.5–6.5 (m, aryl protons), 4.55 (m, C*H*, CHMePh), 3.30 (t br, ^3J(P,H) = 7.0 Hz, *Me*, N–Me), 2.94 (dd, ^3J(P,H) = 16.0, 6.0 Hz, *Me*, N–Me), 1.33 (s br, *Me*, CHMePh). $^{31}P\{^1H\}$ NMR ($CDCl_3$, 162 MHz): 149.9 (m), 143.0 (m), [diphosphazane bearing phenoxy substituents in bridging mode], 105.1 (m), 103.3 (m) [diphosphazane bearing phenoxy substituents in chelating mode], 85.0 (s br), 81.4 (d), 78.7 (d, ^2J(P,P) = 71.3 Hz) [diphosphazane bearing phenyl substituents in chelating mode]. The ^{31}P–^{31}P COSY spectrum of the sample showed the following correlations: (a) cross-peaks between the resonances centered at 105.1 and 81.4 ppm; (b) cross-peaks between the resonances at δ 103.3 and 85.0 as well as 78.7 ppm and (c) cross-peaks between the resonances at 149.9 and 143.0 ppm but no cross-peaks to any other resonances. These correlations indicate the presence of a four spin system. Based on these results and comparison of the NMR chemical shifts (see Table 2), one of the components of this mixture was tentatively formulated as $[Ru_3(\mu_3\text{-}S)_2(CO)_5\{\kappa^2\text{-}P,P\text{-}(PhO)_2PN(Me)P(OPh)_2)\}\{\kappa^2\text{-}P,P\text{-}Ph_2PN(R)PPh_2\}]$ (R = (*S*)-*CHMePh). Attempts to obtain a pure compound from this material by fractional crystallization were unsuccessful.

2.1.12. Reaction of $[Ru_3(\mu_3\text{-}S)(\mu_3\text{-}CO)(CO)_7\{\mu\text{-}P,P\text{-}(PhO)_2PN(Me)P(OPh)_2\}]$ (**9**) with $Ph_2PN((S)\text{-}*CHMePh)P(S)Ph_2$

$Ph_2PN((S)\text{-}*CHMePh)P(S)Ph_2$ (0.041 g, 7.82×10^{-5} mol) and Me_3NO (0.006 g, 9.00×10^{-5} mol) were added to a toluene (20 cm^3) solution of cluster **9** obtained from the reaction of $Ru_3(CO)_{12}$ with **L⁶**. The mixture was heated under reflux for 1 h. Solvent was evaporated; the residue was dissolved in dichloromethane (2 cm^3) and subjected to preparative scale thin-layer chromatography [dichloromethane–petroleum ether (b.p. 60–80 °C) (1:1 v/v) as eluant] to isolate a solid which displayed the following spectroscopic features.

IR (neat, ν_{CO} cm^{-1}): 2016(m), 1989(s), 1948(s). ^1H NMR ($CDCl_3$, 400 MHz): 7.9–6.6 (m, aryl protons), 4.65 (m, C*H*, CHMePh), 3.21 (t, ^3J(P,H) = 7.0 Hz, *Me*, N–Me), 1.10 (d, ^3J(H,H) = 7.0 Hz, *Me*, CHMePh). $^{31}P\{^1H\}$ NMR ($CDCl_3$, 162 MHz): 143.0 (m), 132.0 (m) [diphosphazane bearing phenoxy substituents in bridging mode], 78.0−72.0 (m), 68.0 (d) [diphosphazane bearing phenyl substituents in chelating mode].

Attempts to obtain a pure compound from this material by fractional crystallization were unsuccessful. One of the components of this mixture was tentatively formulated as $[Ru_3(\mu_3\text{-}S)_2(CO)_5\{\mu\text{-}P,P\text{-}(PhO)_2PN(Me)\text{-}P(OPh)_2)\}\{\kappa^2\text{-}P,P\text{-}Ph_2PN(R)PPh_2\}]$ (R = (*S*)-*CHMePh) from the observed ^{31}P chemical shifts.

2.2. X-ray crystallography

The crystals were mounted on a glass fiber and the intensity data for all the clusters were obtained at room temperature from a Bruker SMART APEX CCD diffractometer equipped with fine focus 1.75 kW sealed tube Mo Kα X-ray source with increasing ω (width of 0.3° per frame) at a scan speed of n s/frame (n = 15 for **1**, n = 10 for **3**, n = 9 for **7**, n = 15 for **9**, n = 5 for **10** and n = 6 for **11**). The SMART [25a] software was used for cell-refinement and data acquisition and the SAINT [25b] software was used for data reduction. Lorentzian and polarization corrections were made on the intensity data. An absorption correction was made on the intensity data using the SADABS [25c] program. Pertinent crystallographic data are summarized in Table 3. All the structures were solved using SHELXTL [25d] and the WinGX graphical user interface [26]. Least-square

Table 3
Details of X-ray crystallographic data collection for the cluters **7**, **9**, **10** and **11**

	7 · CH_2Cl_2	**9**	**10**	**11** · $0.5C_6H_6$ · H_2O
Empirical formula	$C_{36}H_{27}NO_9P_2S_2Ru_4.CH_2Cl_2$	$C_{33}H_{23}NO_{12}P_2SRu_3$	$C_{55}H_{46}N_2O_{13}P_4S_2Ru_3$	$C_{34}H_{23}NO_{13}P_2S_2Ru_4.0.5C_6H_6.H_2O$
Formula weight	1232.85	1022.73	1434.15	1240.94
Crystal system, Space group	Triclinic, $P\bar{1}$	Triclinic, $P\bar{1}$	Monoclinic, $P2_1/n$	Monoclinic, $C2/c$
Unit cell dimensions				
a (Å)	12.979(3)	11.390(11)	11.973(3)	24.778(5)
b (Å)	13.138(3)	11.507(11)	25.117(7)	17.034(3)
c (Å)	15.324(3)	15.057(14)	20.249(5)	22.335(4)
α (°)	81.351(3)	78.761(13)		
β (°)	66.286(3)	77.447(14)	104.735(5)	90.138(4)°
γ (°)	63.586(3)	79.832(15)		
Volume (Å^3)	2141(1)	1871(3)	5889(3)	9427(3)
Z	2	2	4	8
Density (calcd) (mg/mm^3)	1.912	1.816	1.618	1.749
Absorption coefficient (mm^{-1})	1.733	1.398	1.002	1.473
Maximum and minimum transmission	0.9383 and 0.7617	0.9793 and 0.4630	0.9073 and 0.5788	0.6972 and 0.4850
$F(000)$	1204	1004	2872	4856
Crystal size, (mm)	$0.300 \times 0.083 \times 0.070$	$0.650 \times 0.130 \times 0.020$	$0.613 \times 0.203 \times 0.099$	$0.540 \times 0.070 \times 0.040$
θ range for data collection	1.45–27.6°	1.82–26.0°	1.32–27.0°	1.45–27.5°
Index ranges	$-17 \leqslant h \leqslant 16$, $-17 \leqslant k \leqslant 16$, $-20 \leqslant l \leqslant 19$	$-14 \leqslant h \leqslant 14$, $-14 \leqslant k \leqslant 13$, $-18 \leqslant l \leqslant 19$	$-15 \leqslant h \leqslant 15$, $-32 \leqslant k \leqslant 31$, $-26 \leqslant l \leqslant 26$	$-31 \leqslant h \leqslant 31$, $-21 \leqslant k \leqslant 22$, $-29 \leqslant l \leqslant 29$
Reflections collected	25,222	19,082	47,991	40,858
Independent reflections [R_{int}]	9956[0.0292]	7492[0.0311]	12,891[0.0638]	11,121[0.0898]
Refinement method	Full-matrix least-squares on F^2	Full-matrix least-squares on F^2	Full-matrix least-squares on F^2	Full-matrix least-squares on F^2
Data/restraints/parameters	9956/0/622	7492/0/561	12,891/0/712	11,121/0/525
Goodness-of-fit on F^2	1.000	1.106	0.933	1.064
Final R indices [$I > 2\sigma(I)$]	$R_1 = 0.0306$, $wR_2 = 0.0796$	$R_1 = 0.0449$, $wR_2 = 0.1018$	$R_1 = 0.0389$, $wR_2 = 0.0637$	$R_1 = 0.0680$, $wR_2 = 0.1140$
R indices all data	$R_1 = 0.0421$, $wR_2 = 0.0839$	$R_1 = 0.0586$, $wR_2 = 0.1088$	$R_1 = 0.0661$, $wR_2 = 0.0688$	$R_1 = 0.1399$, $wR_2 = 0.1309$
Largest different peak and hole (e Å^{-3})	0.878 and −0.667	1.260 and −0.687	0.460 and −0.460	0.794 and −0.559

refinements were performed by the full-matrix method with SHELXL-97 [27]. All non-hydrogen atoms were refined anisotropically and hydrogen atoms were refined isotropically. The solvent molecules in **3** (dichloromethane) and **11** (water oxygen) were disordered and were thus refined isotropically with shared occupancy factors; the carbon atoms of the solvent benzene in **11** were refined isotropically.

3. Results and discussion

3.1. Synthesis of diphosphazane mono- and dichalcogenides and their NMR spectra

The diphosphazane mono- and dichalcogenides are prepared by the treatment of the respective diphosphazane with elemental chalcogen (S_8 or Se) in the appropriate ratio as reported in the literature [17b,28]. The diphosphazane chalcogenides $Ph_2PN((S)$-*$CHMePh)P(Se)Ph_2$ (**L**^{4}) [22] and $Ph_2P(S)N((S)$-*$CHMePh)P(S)Ph_2$ (**L**^{7}) [23] are known compounds. The synthesis of the new diphosphazane chalcogenides **L**^{5}, **L**^{6}, **L**^{8} and **L**^{9} is shown in Scheme 1. The reaction of a diphosphazane that bears a strong π-acceptor phosphorus $(PhO)_2PN(Me)P(OPh)_2$ (**L**^{3}) with one equivalent of elemental sulfur in boiling acetonitrile affords the diphosphazane monosulfide $(PhO)_2PN(Me)P(S)(OPh)_2$ (**L**^{6}). During the synthesis of the known diphosphazane disulfide $Ph_2P(S)N((S)$-*$CHMePh)P(S)Ph_2$ (**L**^{7}) [23], we find that the reaction also yields the disulfide $Ph_2P(S)N(H)P(S)Ph_2$ (see Section 2). Evidently, N–C bond rupture occurs during the oxidation of the trivalent phosphorus by the chalcogen. Recently, Manso et al. [23] investigated the reaction of **L**^{7} with $[Rh(1,5\text{-}COD)(\mu\text{-}Cl)]_2$ in the presence of $AgBF_4$ in which N–C bond rupture occurs to yield the complex, $[Rh(1,5\text{-}COD)\{\kappa^2\text{-}S,S\text{-}Ph_2P(S)N(H)P(S)Ph_2\}]BF_4$. The diphosphazane chalcogenides **L**^{5}–**L**^{9} were characterized by elemental analyses, melting point and NMR spectroscopic techniques (see Table 1).

The ^{31}P chemical shift of the pentavalent phosphorus in the diphosphazane mono- and dichalcogenides lies in the region ~67–70 ppm. For the monoselenides, $Ph_2P(Se)N(R)PPh_2$ [R = (*S*)-*CHMePh (**L**^{4}) or $CHMe_2$ (**L**^{5})], the ^{31}P chemical shifts of the pentavalent phosphorus lie downfield as compared to the parent diphosphazane (**L**^{1} or **L**^{2}). On the other hand, the ^{31}P chemical shift of the pentavalent phosphorus in **L**^{6} is upfield shifted [$\Delta\delta = \delta_P$ (chalcogenide derivative) – δ_P (parent diphosphazane) = − 75.5] compared to the trivalent phosphorus. This reverse trend may be related to the strong π-acceptor character of the phosphorus in **L**^{6}, which is also reflected in the large coupling constant between the two phosphorus nuclei. The ^{1}H NMR spectrum (C_6D_6) of **L**^{6} shows a doublet of doublets for the N(Me) protons. The ^{31}P NMR spectra of the diphosphazane dichalcogenides $Ph_2P(E)N(CHMe_2)P(E)Ph_2$ [E = S (**L**^{8}) or Se (**L**^{9})] display a broad singlet at ~68.0 ppm.

3.2. Reactivity of *L*^{4} and *L*^{5} towards $Ru_3(CO)_{12}$

The reaction of $Ru_3(CO)_{12}$ with **L**^{4} in toluene in the presence of Me_3NO yields a mixture of several products of which only two ruthenium containing species **1** and **2** could be isolated by TLC (Scheme 2). Compound **1** is the diphosphazane bridged selenium bicapped tetraruthenium cluster, $[Ru_4(\mu_4\text{-}Se)_2(CO)_8(\mu\text{-}CO)\{\mu\text{-}P,P\text{-}Ph_2PN((S)\text{-}*CHMePh)PPh_2\}]$ as revealed by X-ray crystallography (see Sections 2.2 and 5). The ^{31}P NMR spectrum of **1** displays a singlet that lies very much downfield as compared to the ^{31}P chemical shift of the free ligand [$\Delta\delta = \delta_P$ (complex)$-\delta_P$ (parent diphosphazane) = +30.6] (see Table 2). The ^{13}C NMR spectrum displays a broad resonance at 202.9 ppm and a singlet at 197.6 ppm for the metal bound carbonyls.

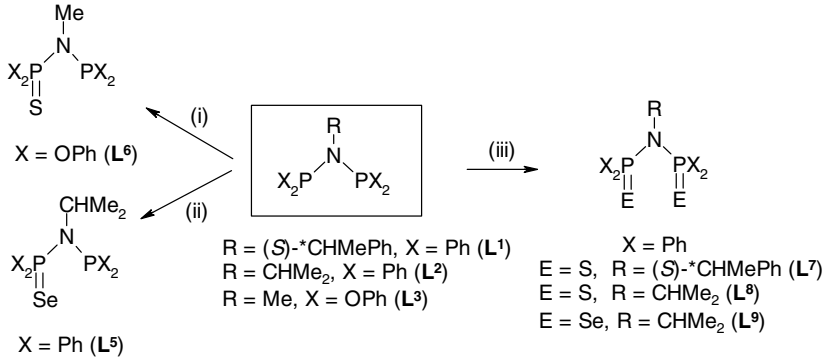

(i) 1/8 S_8, MeCN, 85 °C, 10h
(ii) 1/8 Se_8, THF, 25 °C, 18h
(iii) 2 eq. E, [THF, 65 °C, 8h (for **L**^{7}), Benzene, 80 °C, 1d (for **L**^{8} and **L**^{9})]

Scheme 1. Synthesis of various diphosphazane mono- and di-chalcogenides.

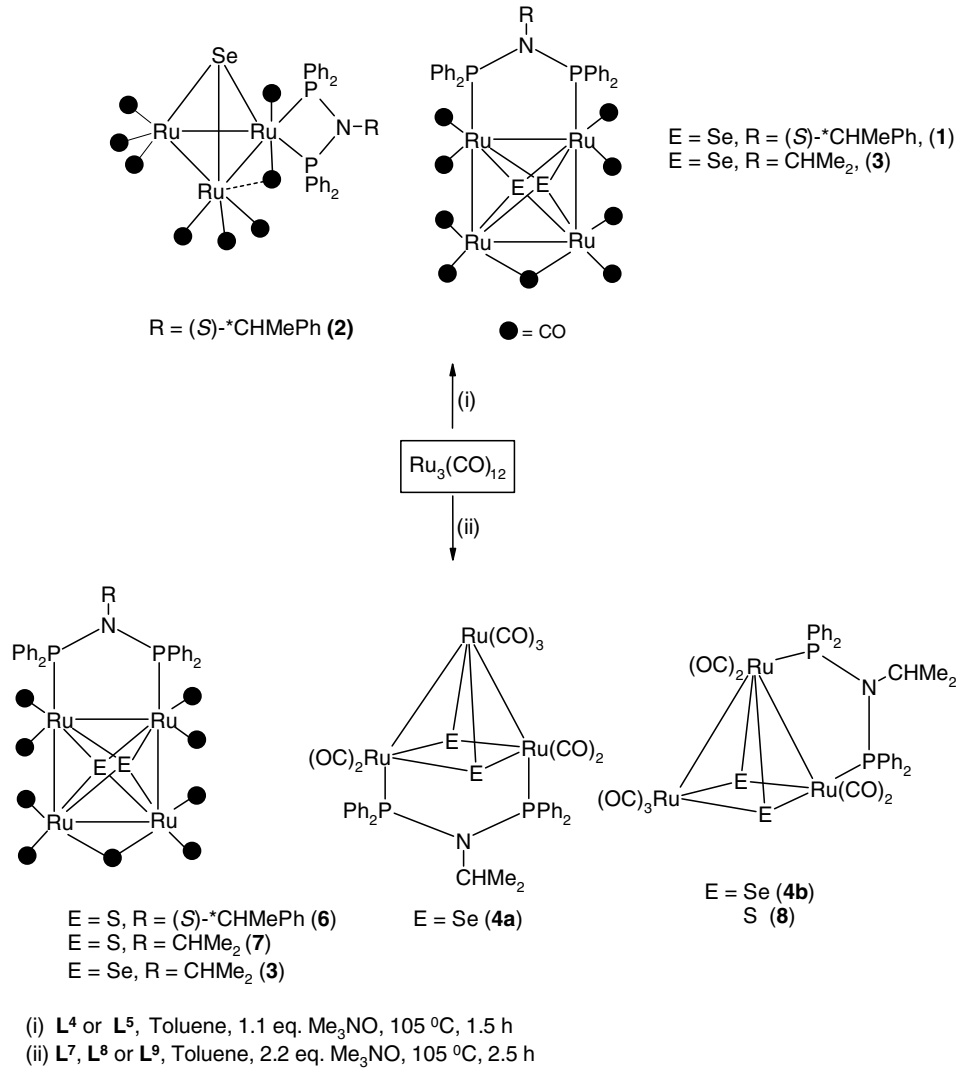

Scheme 2. Reactions of $Ru_3(CO)_{12}$ with diphosphazane mono- and dichalcogenides.

Cluster **2** is assigned the chelated *arachno* structure, $[Ru_3(CO)_7(\mu_3\text{-Se})(\mu_{sb}\text{-CO})\{\kappa^2\text{-P,P-Ph}_2PN((S)\text{-*CHMePh})PPh_2\}]$ (**2**) [$\Delta\delta = +13.4$] by comparison of the NMR chemical shifts and carbonyl stretching frequencies in its infrared spectrum with the data reported for the sulfur analogue, the structure of which has been confirmed by X-ray crystallography [17b].

The reaction of $Ph_2PN(CHMe_2)P(Se)Ph_2$ ($\mathbf{L^5}$) with $Ru_3(CO)_{12}$ results in the formation of several products of which the selenium bicapped tetraruthenium cluster **3** is the major one. The structure of **3** has been confirmed by single crystal X-ray diffraction (see below). The other two products **4** and **5** could be characterised by spectroscopic data only. The ^{31}P NMR spectrum of **4** displays a singlet and two doublets (11:1 ratio) that may be ascribed to the presence of two isomers (**4a** and **4b**) in solution. A similar feature is observed in the case of the *nido* clusters, $[M_3(CO)_7(\mu_3\text{-E})_2\{\mu\text{-P,P-diphosphine}\}]$ (diphosphine = dppm [13b], dppe [13a], dppa [17a]). The ratio of the intensities in the ^{31}P NMR spectrum of **4** indicates that the isomer in which the bridging diphosphine occupies the basal sites (**4a**) is favored presumably because of less steric repulsion experienced in this arrangement. Cluster **5** displays a singlet at 82.5 ppm indicating that the diphosphazane adopts a bridging mode of coordination and is probably a diruthenium species. Attempts to crystallize **4** and **5** were unsuccessful as the products degraded slowly. Complex **3** is also obtained from the reaction between the diselenide $\mathbf{L^9}$ and $Ru_3(CO)_{12}$ (see below).

3.3. Reactivity of diphosphazane dichalcogenides L^7–L^9 towards $Ru_3(CO)_{12}$

The reaction of $Ru_3(CO)_{12}$ with diphosphazane dichalcogenides ($\mathbf{L^7}$–$\mathbf{L^9}$) in boiling toluene in the presence of Me_3NO yield mainly the diphosphazane bridged chalcogen bicapped tetraruthenium clusters,

$[Ru_4(\mu_4\text{-}E)_2(CO)_8\ (\mu\text{-}CO)\{\mu\text{-}P,P\text{-}Ph_2PN(R)PPh_2\}]$ [R = (*S*)-*CHMePh, E = S (**6**); R = $CHMe_2$, E = S (**7**); R = $CHMe_2$, E = Se (**3**)], respectively. The clusters **4b** (see previous section) and **8** are also isolated from the reactions of $Ru_3(CO)_{12}$ with $\mathbf{L^9}$ and $\mathbf{L^8}$, respectively. The IR and NMR data for the clusters are given in Table 2. The structures of the clusters **3** and **7** were established by single crystal X-ray diffraction studies (see Sections 2.2 and 5). The ^{31}P NMR spectrum of **3** or **7** shows a singlet for the magnetically equivalent bridging phosphorus nuclei. An absorption at ~1810 cm^{-1} in the infrared spectrum is assigned to the bridging carbonyl ligand. The ^{31}P NMR spectra of **4b** and **8** exhibit two doublets. Attempts to obtain single crystals of **4b** and **8** were unsuccessful. Based on the IR spectroscopic data and ^{31}P NMR chemical shifts, we tentatively assign a structure in which the diphosphazane acts as a bridging ligand.

3.4. Reactivity of the diphosphazane monosulfide L^6 towards $Ru_3(CO)_{12}$

The oxidative decarbonylation of $Ru_3(CO)_{12}$ by Me_3NO in the presence of $\mathbf{L^6}$ proceeds through a different pathway to yield two products **9** and **10** corresponding to single and double oxidative transfer of sulfur respectively (Scheme 3). Clusters **9** and **10** were separated by thin layer chromatography and their structures determined by X-ray crystallography (Figs. 1 and 2). A singlet is observed in the $^{31}P\{^1H\}$ NMR spectrum of cluster **9**. The infrared spectrum of **9** shows a band at 1701 cm^{-1} for the triply bridging carbonyl group. The ^{13}C NMR spectrum displays resonances at 199.0 and 194.9 ppm, which can be assigned to the metal bound carbonyl ligands. Crystallization of the compound from a mixture of benzene and petroleum ether over a period of two months at ambient temperature gave **9** as thin yellow needle-shaped crystals suitable for X-ray diffraction. In addition, a tiny quantity of dark red crystals was also obtained. A single crystal X-ray study was carried out on the dark red crystals; the structure was found to be the sulfur bicapped tetraruthenium *closo* octahedral cluster **11** (Fig. 3).

The reactions of diphosphazane monosulfides $Ph_2PN(R)P(S)Ph_2$ (R = (*S*)-*CHMePh or $CHMe_2$) with $Ru_3(CO)_{12}$ give sulfur monocapped triruthenium clusters, $[Ru_3(\mu_3\text{-}S)(\mu_{sb}\text{-}CO)(CO)_7\{\kappa^2\text{-}P,P\text{-}Ph_2PN(R)PPh_2\}]$ in which the diphosphazane acts as a chelating ligand [17b]. The reaction of the cluster $[Ru_3(_3\text{-}S)(\mu_{sb}\text{-}CO)(CO)_7\{\kappa^2\text{-}P,P\text{-}Ph_2PN((S)\text{-}*CHMePh)PPh_2\}]$ (**A**) with $(PhO)_2PN(Me)P(S)(OPh)_2$ ($\mathbf{L^6}$) in boiling toluene in the presence of Me_3NO as decarbonylating agent gave a mixture of products which could not be separated and isolated in a pure state. However, based on ^{31}P–^{31}P COSY spectrum and observed ^{31}P chemical shifts (see Section 2), one of the products is tentatively identified as $[Ru_3(\mu_3\text{-}S)_2(CO)_5\{\kappa^2\text{-}P,P\text{-}(PhO)_2PN(Me)P(OPh)_2\}\{\kappa^2\text{-}P,P\text{-}Ph_2PN((S)\text{-}*CHMePh)PPh_2\}]$ in which both the diphosphazane ligands adopt chelating mode of coordination.

The reaction of $[Ru_3(\mu_3\text{-}S)(\mu_3\text{-}CO)(CO)_7\{\mu\text{-}P,P\text{-}(PhO)_2PN(Me)P(OPh)_2\}]$ (**9**) with the diphosphazane monosulfide, $Ph_2PN((S)\text{-}*CHMePh)P(S)Ph_2$ in boiling toluene in the presence of Me_3NO as decarbonylating

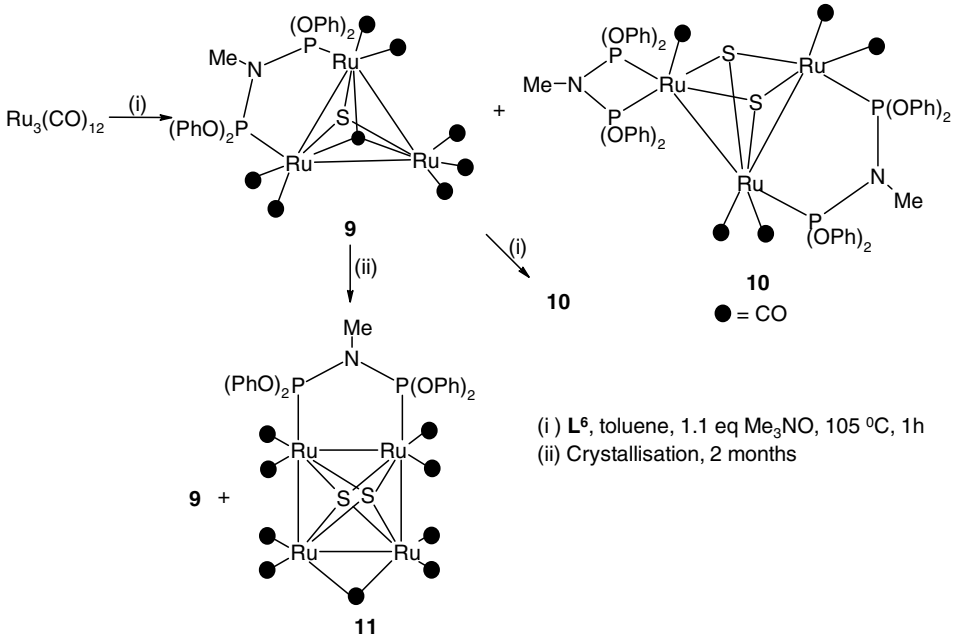

Scheme 3. Reactivity of diphosphazane monosulfide $(PhO)_2PN(Me)P(S)(OPh)_2$ ($\mathbf{L^6}$) towards $Ru_3(CO)_{12}$.

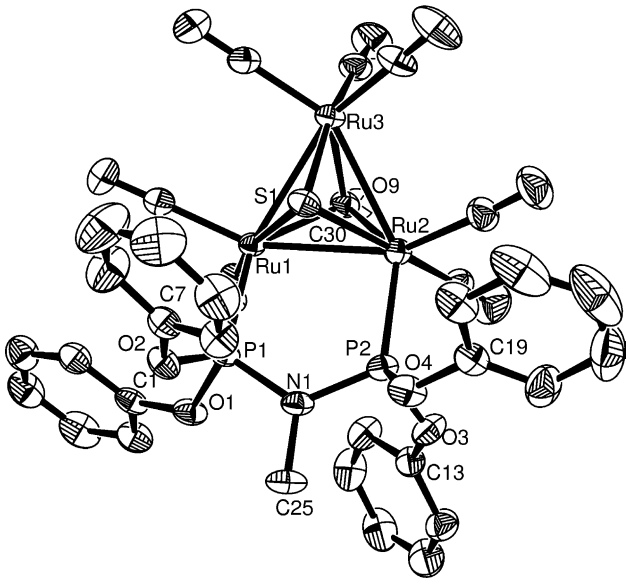

Fig. 1. An ORTEP view of the molecular structure of $[Ru_3(CO)_7(\mu_3\text{-}S)(\mu_3\text{-}CO)\{\mu\text{-}P,P\text{-}(PhO)_2PN(Me)P(OPh)_2\}]$ (**9**). Thermal ellipsoids are drawn at 30% probability level. Hydrogen atoms are not shown for clarity.

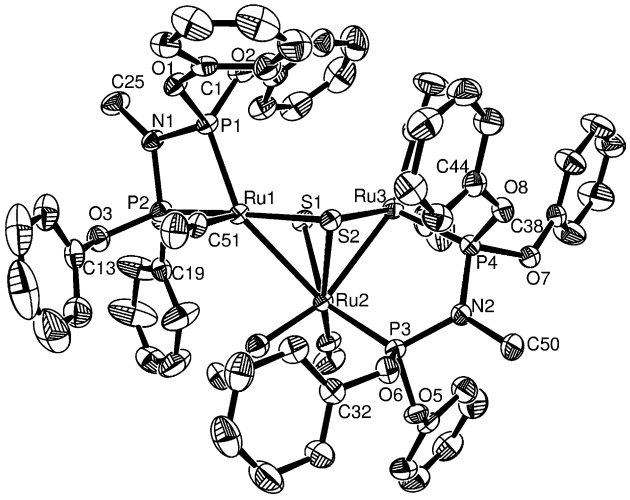

Fig. 2. An ORTEP view of the molecular structure of $[Ru_3(CO)_5(\mu_3\text{-}S)_2\{\mu\text{-}P,P\text{-}(PhO)_2PN(Me)P(OPh)_2\}\{\kappa^2\text{-}P,P\text{-}(PhO)_2PN(Me)P(OPh)_2\}]$ (**10**). Thermal ellipsoids are drawn at 30% probability level. Hydrogen atoms are not shown for clarity.

agent also gave a mixture of products which could not be separated and isolated in a pure form. Based on IR and NMR spectroscopic data (see Section 2), one of the products can be tentatively identified as $[Ru_3(\mu_3\text{-}S)_2(CO)_5\{\mu\text{-}P,P\text{-}(PhO)_2PN(Me)P(OPh)_2\}\{\kappa^2\text{-}P,P\text{-}Ph_2PN((S)\text{-}*CHMePh)PPh_2\}]$ in which the incoming diphosphazane adopts a chelating mode of coordination. Further reaction of $[Ru_3(\mu_3\text{-}S)(\mu_{sb}\text{-}CO)(CO)_7\{\kappa^2\text{-}P,P\text{-}Ph_2PN((S)\text{-}*CHMePh)PPh_2\}]$ (**A**) with the diphosphazane monosulfide $Ph_2PN((S)\text{-}*CHMePh)P(S)Ph_2$ or $Ph_3P(S)$ in the presence

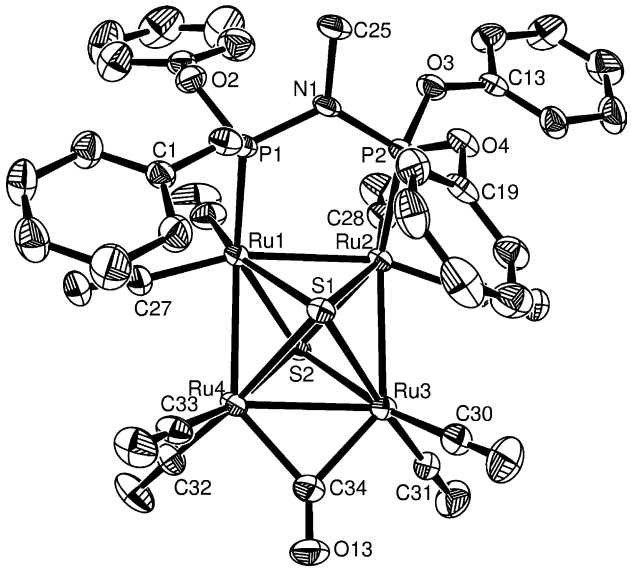

Fig. 3. An ORTEP view of the molecular structure of $[Ru_4(CO)_8(\mu_4\text{-}S)_2(\mu\text{-}CO)\{\mu\text{-}P,P\text{-}(PhO)_2PN(Me)P(OPh)_2\}]$ (**11**). Thermal ellipsoids are drawn at 30% probability level. Hydrogen atoms and lattice held solvent molecules (benzene and water) are not shown for clarity.

of Me_3NO did not proceed and the starting material (**A**) was recovered unchanged.

3.5. NMR spectrum and dynamic behavior of *10*

Cluster **10** represents the first example of a chalcogen bridged carbonyl cluster bearing two bidentate phosphorus ligands in two different coordination modes. As evident from the structure of **10** (Fig. 2), all the four phosphorus nuclei are magnetically non-equivalent. Hence, one would expect the ^{31}P NMR spectrum to consist of 32 lines. But the actual spectrum is more complicated (Fig. 4). A homonuclear ^{31}P–^{31}P COSY experiment shows that the complexity is due to the presence of two isomers (1:4 ratio) each giving rise to an AMRX spin system. The COSY spectrum is illustrated in Fig. 5. The ^{31}P chemical shifts and coupling constants for only the major isomer (**10**) could be determined accurately; for the minor isomer (**10a**) only the chemical shifts could be determined as the resonances were not well resolved. The values calculated directly from the spectrum for **10** agree closely with those obtained by computer simulation using the LEQUOR program [29]. The ^{31}P NMR spectrum (recorded in acetone-d_6) does not show any change in the temperature range −90 to +50 °C.

The assignment of the ^{31}P NMR chemical shifts for the major isomer **10** is based on the following two trends noted in the literature: (a) the ^{31}P chemical shifts of bridging diphosphazanes are downfield shifted compared to those of the chelating ones [17b] (also see data for compounds given in Table 2) (b) within a chelating diphosphine, the chemical shift of the phosphorus that

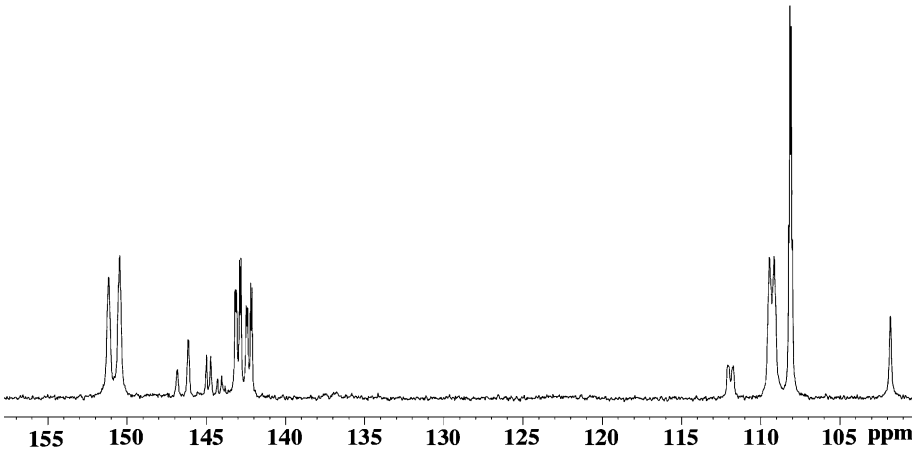

Fig. 4. The ^{31}P NMR spectrum (162 MHz, $CDCl_3$, 20 °C) of **10**.

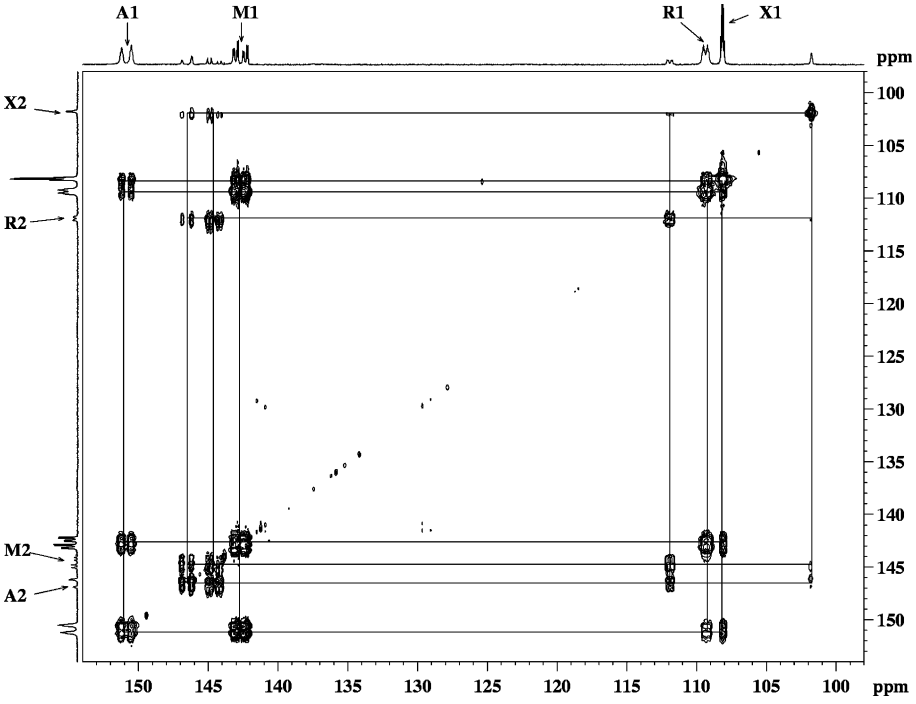

Fig. 5. The ^{31}P–^{31}P COSY spectrum (162 MHz, $CDCl_3$, 20 °C) of **10**.

occupies the axial position lies downfield compared to that present at the equatorial position [13d]. Based on these two correlations, the ^{31}P resonances centered at 151.1(dt, P_{A1}) and 142.7(ddd, P_{M1}) ppm are assigned to the phosphorus nuclei of the bridging diphosphazane and those centered at 110.3(dt, P_{R1}) and 109.4(q, P_{X1}) are assigned to the axial and equatorial phosphorus nuclei of the chelating diphosphazane, respectively. Considering the X-ray crystal structure and the relevant torsion angles (see Fig. 2 and the X-ray crystal structure section), the phosphorus nuclei of the bridging diphosphazane located at the apex of the square pyramid [P(3) in Fig. 2] would be expected to have three widely different coupling constants [^2J (P,P), $^3J(P,P)_{trans}$, $^3J(P,P)_{cis}$]. The other phosphorus [P(4) in Fig. 2] present at the base of the square pyramid would also have three coupling constants [^2J(P,P), ^4J(P,P),^4J(P,P)], of which the two long-range coupling constants will be weak (probably equal in magnitude). Therefore the resonance centered at δ 142.7(ddd) is assigned to the phosphorus at the apex of the square pyramid and that at δ 151.1(dt) is assigned to the phosphorus at the base of the square pyramid. Fig. 6 shows the assignment of ^{31}P chemical shifts to the phosphorus nuclei in **10** and **10a**.

A homonuclear ^{31}P–^{31}P phase-sensitive NOESY experiment, (Fig. 7) reveals that the two isomers undergo

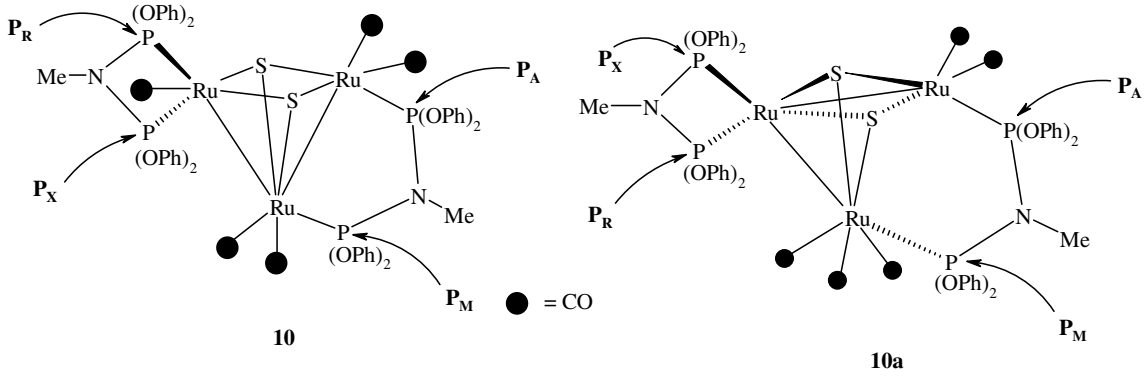

Major isomer 10

P_A, 151.1 (dt, ^2J(A-M) = 112.4 Hz, ^4J(A-R) = ^4J(A-X) = 13.8 Hz)
P_M, 142.7 (ddd, ^2J(M-A) = 112.4 Hz, ^3J(M-R) = 48.2 Hz, ^3J(M-X) = 13.8 Hz)
P_R, 109.3 (dt, ^3J(R-M) = 48.2 Hz, ^4J(R-A) = ^2J(R-X) = 16.1 Hz)
P_X, 108.1 (q, ^2J(X-R) = ^3J(X-M) = ^4J(X-A) = 13.8 Hz)

Minor isomer 10a

P_A, 146.5
P_M, 144.5
P_R, 111.9
P_X, 101.8

Fig. 6. Assignment of ^{31}P chemical shifts to phosphorus nuclei in the two isomers **10** and **10a**.

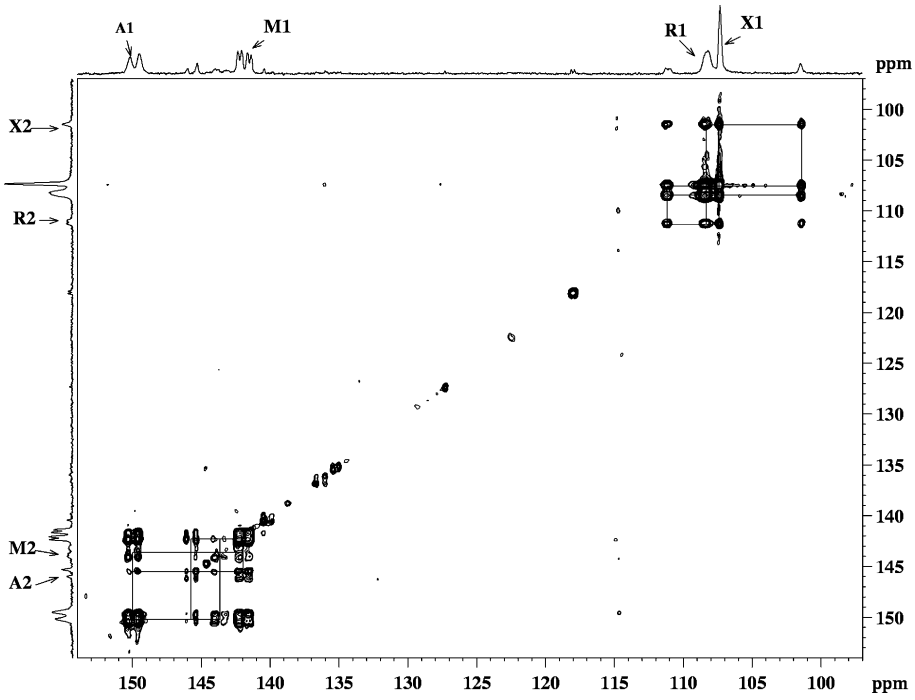

Fig. 7. The ^{31}P–^{31}P phase sensitive NOESY spectrum (162 MHz, $CDCl_3$, 20 °C) of **10**.

exchange in solution. The exchange process can be explained on the basis of a reversible skeletal rearrangement brought about by the migration of a Ru–Ru bond across the ruthenium triangle [13a] as shown in Scheme 4. Depending on which of the two Ru–Ru bonds (Ru1–Ru2 or Ru2–Ru3) migrates to the basal plane of the square pyramid linking the two non-bonded Ru atoms (Ru1 and Ru3), different exchange behavior would be observed. Isomerization via path **A** would result in the exchange of P_{A1}, P_{M1}, P_{R1} and P_{X1} with P_{A2}, P_{M2}, P_{X2} and P_{R2}, respectively. This pathway leads to the isomer (**10a**) which differs significantly from the solid-state structure in that the bridging diphosphazane links the two non-bonded ruthenium atoms in the basal plane. Isomerisation via path **B** would result in the exchange of P_{A1}, P_{M1}, P_{R1} and P_{X1} with P_{M3}, P_{A3}, P_{X3} and P_{R3}, respectively. The isomer obtained in this way (**10′**) is similar to **10** and differs only in the number of

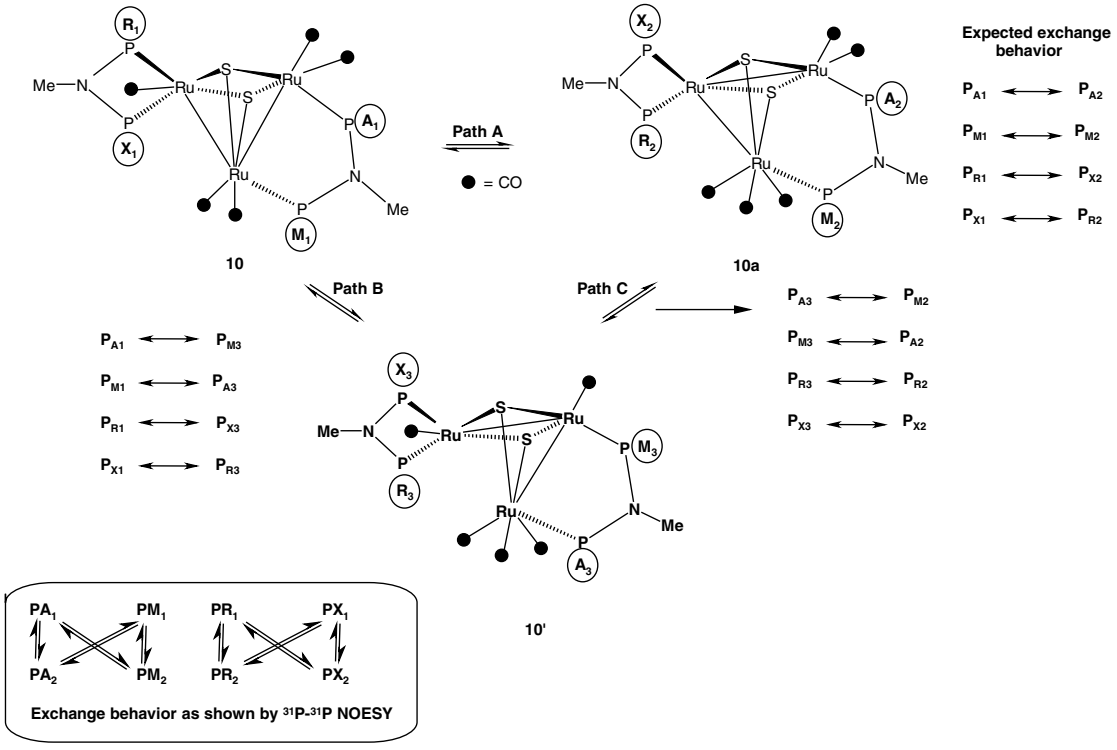

Scheme 4. Reversible skeletal rearrangements occurring in the cluster $[Ru_3(\mu_3\text{-}S)_2(CO)_5\{\kappa^2\text{-}P,P\text{-}(PhO)_2PN(Me)P(OPh)_2\}\{\mu\text{-}P,P\text{-}(PhO)_2PN(Me)\text{-}P(OPh)_2\}]$ (**10**).

carbonyls at the ruthenium centers. Because of the similarity in the structures of **10** and **10′**, the ^{31}P chemical shifts of the phosphorus nuclei in **10′** (P_{A3}, P_{M3}, P_{R3}, P_{X3}) would be close to those of **10** (P_{A1}, P_{M1}, P_{R1}, P_{X1}) and hence separate resonances for **10′** are not observed. This supposition is supported by the observation of the exchange peaks A_1–M_3, M_1–A_3, R_1–X_3 and X_1–R_3 in the ^{31}P–^{31}P phase-sensitive NOESY spectrum (Fig. 7) at the same position as the correlation peaks observed for the A_1–M_1 and R_1–X_1 in the COSY spectrum (Fig. 5). The direct exchange peaks observed for the phosphorus nuclei of the chelating diphosphazane (R_1 exchanging with R_2, X_1 exchanging with X_2) can be accounted for by the isomerisation of **10′** to **10a** via path C. The observed exchange behavior (see Scheme 4) clearly shows that isomerization occurs by all the three pathways; however, among the three possible isomers as noted above, resonances of only two distinct isomers are observed in the ^{31}P NMR spectrum.

The ^1H NMR spectrum of **10** displays only three triplets in the ratio 5:4:1 for the methyl protons attached to nitrogen (two triplets are expected for each isomer). The downfield triplet is assigned to the methyl protons of the bridging diphosphazane of both the isomers based on heteronuclear ^{31}P–^1H COSY experiment. The other two triplets arise from the methyl protons of the chelating diphosphazane of the two isomers. A ^1H–^1H ROESY spectrum shows exchange peaks between the two triplets that correspond to the methyl protons of the chelating diphosphazane of the two isomers.

3.6. Crystal and molecular structures of the tetraruthenium clusters *1*, *3*, *7* and *11*

The structures of the clusters **1**, **3**, **7** and **11** as revealed by X-ray crystallography show an octahedral arrangement of four ruthenium atoms and two chalcogens in which the four metals form the square plane. The diphosphazane adopts a bridging mode of coordination and lies *trans* to the doubly bridging carbonyl ligand. All these clusters are isostructural and show similar trends in their structural parameters. For a comparison of the structural features of these tetraruthenium clusters, selected data of **7** and **11** only are included here (see Table 4). The data for the clusters **1** and **3** are given in Section 5. The molecular structure of **11** is shown in Fig. 3. The Ru–Ru edge bridged by the diphosphazane in these *closo* octahedral clusters is shorter (~0.08–0.13 Å) than the other two edges that do not contain a bridging ligand. It is also shorter (~0.04–0.07 Å) than the edge bridged by the carbonyl ligand reflecting the short span angle of the diphosphazane. Such a trend in the bond lengths is also observed in dppa $[Ph_2PN(H)PPh_2]$ (0.08–0.10 and 0.02 Å) clusters, $[Ru_4(\mu_4\text{-}E)_2(\mu\text{-}CO)(CO)_8\{\mu\text{-}P,P\text{-dppa}\}]$ (E = S, Se) [17a]. However, in the dppm $[Ph_2PCH_2PPh_2]$ [13b] analogue,

Table 4
Comparison of structural parameters in the clusters **7**, **9**, **10** and **11**

	7	**9**	**10**	**11**
Bond distances (Å)				
Ru(1)–Ru(2)	2.690(1)[a]	2.769(2)[a]	2.827(1)	2.696(1)[a]
Ru(1)–Ru(4)	2.771(1)	–	–	2.791(1)
Ru(2)–Ru(3)	2.824(1)	2.809(2)	2.722(1)[a]	2.798(1)
Ru(3)–Ru(4)[b]	2.755(1)	2.809(2)	–	2.742(1)
Ru–S(1)$_{\langle ave\rangle}$	2.469(1)	2.370(2)	2.386(1)	2.486(2)
Ru–S(2)$_{\langle ave\rangle}$	2.480(1)	–	2.393(1)	2.468(2)
Ru–P	2.289(1), 2.332(1)	2.263(2), 2.266(2)	2.207(1), 2.272(1)[c] 2.253(1), 2.237(1)[d]	2.249(2) 2.244(2)
P–N$_{\langle ave\rangle}$	1.716(2)	1.673(4)	1.668(2),[c] 1.675(2)[d]	1.670(5)
Ru–C(O)$_{\langle ave\rangle}$	1.876(4)	1.913(5)	1.898(4)	1.878(7)
Ru–C(O)$_{\langle ave\rangle}$ (bridging)	2.044(4)	2.177(5)	–	2.042(7)
C–O(μ)	1.157(4)	1.189(5)	–	1.155(7)
Bond angles (°)				
P–N–P	118.5(1)	121.4(2)	98.6(2),[c] 120.9(2)[d]	122.4(3)
P–N–C	116.8(2) 124.2(2)	119.3(4) 119.2(4)	130.2(2), 130.8(2)[c] 118.9(2), 120.1(2)[d]	118.3(4) 119.2(4)
Ru–C–O(μ)	137.2(3), 138.1(3)	132.1(3) 132.8(4) 131.5(4)	–	137.2(6), 138.4(3)

[a] Edge bridged by diphosphazane.
[b] Edge bridged by carbonyl ligand.
[c] Chelating diphosphazane.
[d] Bridging diphosphazane.

while the edge bridged by the diphosphine is shorter than the other two ''non-bridged'' edges (0.06 Å), the edge bridged by dppm is longer than that bridged by carbonyl ligand (0.02 Å). Though the span angle of dppm (115.2(2)°) is shorter than that of the diphosphazanes used here, this reverse trend in bond distance is probably due to the less π-back bonding to the phosphorus center in dppm as compared to P–N–P analogues. The Ru–P, Ru–E (E = S or Se), Ru–C(O), C–O and P–N distances are unexceptional and are comparable to literature values [13b,17]. The Ru–P bond in cluster **11**, in which the diphosphazane bears a strong π-acceptor phosphorus, is shorter than that in the clusters **1**, **3**, and **7** (see Table 4 and Section 5). The strong π-acceptor nature of the phosphorus in **11** is also responsible for the shortening of P–N bond distance by ∼0.04 Å as compared to **7**. The sum of the angles at nitrogen in this cluster and in all the clusters reported in this paper is close to 360° revealing planar geometry around the nitrogen atom.

The contrast in the cluster skeletal framework of the ''*closo* octahedral'' chalcogen bicapped tetraruthenium clusters, $[Ru_4(\mu_4\text{-}E)_2(\mu\text{-}CO)(CO)_8\{\mu\text{-}P,P\text{-}Ph_2PN(R)PPh_2\}]$ [E = Se, R = (*S*)-*CHMePh (**1**) or E = S, R = $CHMe_2$ (**7**)] with that of the sulfur monocapped ''*arachno* tetrahedral'' triruthenium cluster $[Ru_3(\mu_3\text{-}S)(\mu_{sb}\text{-}CO)(CO)_7\{\kappa^2\text{-}P,P\text{-}Ph_2PN((S)\text{-}*CHMePh)PPh_2\}]$ (**A**) [17b] is noteworthy. The Ru–Ru edges that do not bear a bridging ligand in the clusters **1** or **7** are longer than those in the sulfur monocapped cluster. The edge bridged by the carbonyl ligand in **1** or **7** is shorter (∼0.04–0.06 Å) than that in the monocapped cluster. This shortening can be attributed to the different coordination modes of the bridging carbonyl ligand in the two types of clusters (symmetrically bridging in the clusters **1** and **7**, semi-bridging in the previously reported cluster [17b]). The mean Ru–S distances in cluster **7** is longer (∼0.11 Å) than that in the sulfur monocapped cluster. This indicates an overall expansion of the cluster core upon going from *arachno* tetrahedral to *closo* octahedral framework.

3.7. Crystal and molecular structures of the triruthenium clusters *9* and *10*

The structure of $[Ru_3(\mu_3\text{-}S)(\mu_3\text{-}CO)(CO)_7\{\mu\text{-}P,P\text{-}(PhO)_2PN(Me)P(OPh)_2\}]$ (**9**) (Fig. 1) consists of an isosceles triangle of triruthenium framework with a triply bridging sulfur, a triply bridging carbonyl group and a bridging diphosphazane ligand. This cluster is a 48 electron species, in which the cluster core has a trigonal bipyramidal geometry consisting of 3 ruthenium atoms, a triply bridging sulfur and a triply bridging carbonyl ligand. To the best of our knowledge, there are only two reports on the ''*structural characterization* '' of $[M_3(\mu_3\text{-}E)(\mu_3\text{-}CO)L_9]$ (L = $2e^-$ donor ligand) family of clusters bearing phosphorus donor ligands, viz. $[Os_3(\mu_3\text{-}Se)(\mu_3\text{-}CO)(CO)_7\{\mu\text{-}P,P\text{-}Ph_2PCH_2PPh_2\}]$ [9b] and $[Ru_3(\mu_3\text{-}Se)(\mu_3\text{-}CO)(CO)_7(PPh_3)_2]$ [10b]. Other reports [30] on this family of clusters do not bear phosphorus donor ligands. The bonding parameters are listed in Table 4. The Ru–Ru edge bridged by the diphosphazane is 0.04 Å shorter than the other two edges. The triply bridging sulfur lies at 1.736 Å above the triruthenium plane while the carbonyl group is located at 1.460 Å below the triruthenium plane. There is a slight asymmetry in the coordination of the triply bridging carbonyl and sulfur to the triruthenium core. The triply bridging

sulfur (4 electron donor) is closer to Ru(1) and Ru(3) while the triply bridging carbonyl (2 electron donor) is closer to Ru(2) and is slightly farther from the other two ruthenium centers. The span angle of the diphosphazane is slightly greater than that seen in the other structures reported in this paper and is closer to that in **11**, because of which the Ru–Ru edge bridged by the diphosphazane is longer than that in the clusters **1**, **3** and **7** (see Table 4 and Section 5). The Ru–S distances are shorter than those in the *closo* structures **7** and **11**. The C–O bond distance of the triply bridging carbonyl (1.189(6) Å) is longer than that observed in **1**, **3** and **7** (1.16 Å) and is close to that reported in literature for a triply bridging carbonyl [9b,10b].

The molecular structure of **10** (Fig. 2) represents a 50-electron square pyramidal open *nido* triruthenium cluster that bears two diphosphazane ligands in different coordination modes (one chelating and the other bridging mode of binding). The bite angle at Ru(1) is 68.8° while the span angle of the chelating and bridging diphosphazane units are 98.6° and 120.9°, respectively. The Ru–Ru edge that bears the bridging diphosphazane is 0.1 Å shorter than the other edge. The torsion angles P(1)–Ru(1)–Ru(2)–P(3) and P(2)–Ru(1)–Ru(2)–P(3) [100.6(1)° and −155.9(1)°, respectively] indicate that P(1) is *pseudo-trans* to P(3) while P(2) is *cisoid* to P(3). The presence of two strongly π-accepting phosphorus centers almost *trans* to each other on either side of the Ru(1)–Ru(2) bond elongates it compared to Ru(2)–Ru(3) distance. Hence, there is a considerable shortening of Ru(1)–P(1) bond at the *pseudo-axial* position compared to the other Ru–P distances. The Ru–S bond distances are similar to those in **9** but shorter than those in **11**. Other bond-distances and bond-angles are similar to those observed in other structures. The packing in the lattice consists of a weak hydrogen bond network involving the hydrogen atoms on the phenyl rings and the oxygen atoms of the carbonyl group. The solid-state structure is the favored isomer in solution also because, in this geometry, there is a subtle balance of the π-accepting capability of the phosphorus nuclei present at each ruthenium center. On the other hand, in the minor isomer that exists in solution, the presence of two strongly π-acceptor phosphorus mutually *trans* to each other could probably weaken the cluster framework. At this stage it is worth noting that the solid state structure of the triruthenium dppa cluster, $[Ru_3(\mu_3\text{-}S)_2(CO)_7(\mu\text{-}P,P\text{-}dppa)]$ is the one in which the dppa ligand bridges two non-bonded ruthenium atoms [17a] corresponding to the minor isomer **10a**. The Ru…Ru non-bonded distance in **10** and $[Ru_3(\mu_3\text{-}S)_2(CO)_7(\mu\text{-}P,P\text{-}dppa)]$ are 3.653 and 3.561 Å, respectively. The smaller span angle of the ligand in **10** (120.9) compared to that of the dppa ligand (137.7) in $[Ru_3(\mu_3\text{-}S)_2(CO)_7(\mu\text{-}P,P\text{-}dppa)]$ may be responsible for the bridging of the two bonded ruthenium centers in **10** by the diphosphazane ligand.

When we compare the values of the Ru–Ru edge bridged by the diphosphazane that bears the same diphosphazane ligand as in clusters **9**, **10** and **11**, we find that on going from a trigonal bipyramidal geometry (**9**) to an octahedral geometry (**11**) through the square pyramidal gemometry (**10**), there is a gradual decrease in the Ru–Ru edge bridged by the diphosphazane, a trend that implies a gradual closing of the cluster framework. Concomitantly, the mean Ru–S distance shows a gradual increase along the sequence **9**, **10** and **11**.

4. Conclusions

A variety of chalcogen bridged ruthenium carbonyl clusters have been synthesized from the reaction of $Ru_3(CO)_{12}$ with a range of diphosphazane mono- and dichalcogenides by varying the chalcogen and the π-acceptor capability of the phosphorus centers. In general, it is found that diphosphazane monosulfides bearing a less π-acceptor phosphorus give rise to sulfur monocapped triruthenium clusters in which the diphosphazane adopts a chelating mode of coordination [17b]. On the other hand, diphosphazane monoselenides afford the bicapped tetraruthenium clusters in which the diphosphazane is in bridging mode of coordination in addition to monocapped triruthenium clusters. Diphosphazane dichalcogenides give mainly chalcogen bicapped tetraruthenium clusters as the main products irrespective of the nature of the chalcogen. Diphosphazane monosulfide derived from a diphosphazane bearing a strong π-acceptor phosphorus shows a different type of reactivity. Stepwise sulfur transfer occurs to give successively a sulfur monocapped Ru_3 cluster containing a μ_3-CO and a bridging diphosphazane and a sulfur bicapped Ru_3 cluster containing both chelating and bridging diphosphazane. Preliminary experiments on the synthesis of sulfur bicapped ruthenium carbonyl clusters bearing two different diphosphazane ligands reveal that, at least one of the diphosphazanes should be a strong π-acceptor [e.g. $(PhO)_2PN(Me)P(OPh)_2$]. Monochalcogenides (e.g. $\mathbf{L^4}$, $\mathbf{L^5}$ and $Ph_2PN(R)P(S)Ph_2$) derived from a diphosphazane in which the π-acceptor capability of the phosphorus centers is low do not give a chalcogen bicapped cluster bearing two diphosphazane moieties. Also, irrespective of the nature of the π-acceptor capability of the phosphorus centers in the diphosphazane monosulfide, second sulfur transfer occurs to give a cluster in which the second diphosphazane adopts a chelating mode of coordination.

5. Supplementary material

Crystallographic data for the structures reported in this paper have been deposited with the Cambridge Crystallographic Data Centre as supplementary publication

nos. CCDC-252278 (**1**), -252279 (**3**), -252280 (**7**), -252281 (**9**), -252282 (**10**) and -252283 (**11**) contain the supplementary crystallographic data for this paper. Copies of the data can be obtained free of charge from the Director, CCDC, 12, Union Road, Cambridge, CB2 1EZ, UK (Fax: +44 1223 336033; deposit@ccdc.cam.ac.uk or http://www.ccdc.cam.ac.uk

Acknowledgements

We thank the Department of Science and Technology, New Delhi, India for financial support and for the data collection using the CCD X-ray facility, IISc, Bangalore set up under IRHPA program. We also thank Dr. N. Suryaprakash and Ms. Anu Joy (Sophisticated Instruments Facility, Indian Institute of Science, Bangalore) for simulation of the NMR spectrum of compound **10**.

References

[1] L.C. Roof, J.W. Kolis, Chem. Rev. 93 (1993) 1037–1080.
[2] (a) D. Cauzzi, C. Graiff, G. Predieri, A. Tiripicchio, in: P. Braunstein, L.A. Oro, P.R. Raithby (Eds.), Metal Clusters in Chemistry, vol. I, Wiley-VCH, Weinheim, 1999, pp. 193–208;
(b) C. Graiff, G. Predieri, A. Tiripicchio, Eur. J. Inorg. Chem. (2003) 1659–1668.
[3] S. Dehnen, A. Eichhöfer, D. Fenske, Eur. J. Inorg. Chem. (2002) 279–317.
[4] M.L. Steigerwald, Polyhedron 13 (1994) 1245–1252.
[5] D. Cauzzi, C. Graiff, R. Pattacini, G. Predieri, A. Tiripicchio, S. Kahlal, J.-Y. Saillard, Eur. J. Inorg. Chem. (2004) 1063–1072.
[6] (a) R.D. Adams, J.E. Babin, P. Mathur, K. Natarajan, J.-G. Wang, Inorg. Chem. 28 (1989) 1440–1445;
(b) P. Braunstein, C. Graiff, C. Massera, G. Predieri, J. Rose, A. Tiripicchio, Inorg. Chem. 41 (2002) 1372–1382.
[7] P. Baistrocchi, D. Cauzzi, M. Lanfranchi, G. Predieri, A. Tiripicchio, M.T. Camellini, Inorg. Chim. Acta 235 (1995) 173–183.
[8] (a) R.D. Adams, J.E. Babin, M. Tasi, Inorg. Chem. 25 (1986) 4514–4519;
(b) P. Mathur, B.S. Thimmappa, A. Rheingold, Inorg. Chem. 29 (1990) 4658–4665;
(c) B.F.G. Johnson, T.M. Layer, J. Lewis, A. Martín, P.R. Raithby, J. Organomet. Chem. 429 (1992) C41–C45;
(d) T.M. Layer, J. Lewis, A. Martín, P.R. Raithby, W.-T. Wong, J. Chem. Soc. Dalton Trans. (1992) 3411–3417;
(e) P. Mathur, Md.M. Hossain, R. Rashid, J. Organomet. Chem. 448 (1993) 211–214.
[9] (a) K.A. Azam, G.M.G. Hossain, S.E. Kabir, K.M. Abdul Malik, Md.A. Mottalib, S. Perven, N.C. Sarker, Polyhedron 21 (2002) 381–387;
(b) S.E. Kabir, S. Pervin, N.C. Sarker, A. Yesmin, A. Sharmin, T.A. Siddiquee, D.T. Haworth, D.W. Bennett, K.M. Abdul Malik, J. Organomet. Chem. 681 (2003) 237–249.
[10] (a) W.K. Leong, W.L.J. Leong, J. Zhang, J. Chem. Soc. Dalton Trans. (2001) 1087–1090;
(b) D. Belletti, D. Cauzzi, C. Graiff, A. Minarelli, R. Pattacini, G. Predieri, A. Tiripicchio, J. Chem. Soc. Dalton Trans. (2002) 3160–3163.
[11] D. Belletti, C. Graiff, V. Lostao, R. Pattacini, G. Predieri, A. Tiripicchio, Inorg. Chim. Acta 347 (2003) 137–144.
[12] (a) D. Cauzzi, C. Graiff, C. Massera, G. Predieri, A. Tiripicchio, Inorg. Chim. Acta 300–302 (2000) 471–476;
(b) D. Cauzzi, C. Graiff, C. Massera, G. Predieri, A. Tiripicchio, J. Cluster Sci. 12 (2001) 259–271;
(c) D. Cauzzi, C. Graiff, C. Massera, G. Predieri, A. Tiripicchio, Eur. J. Inorg. Chem. (2001) 721–723.
[13] (a) D. Cauzzi, C. Graiff, M. Lanfranchi, G. Predieri, A. Tiripicchio, J. Organomet. Chem. 536–537 (1997) 497–507;
(b) D. Cauzzi, C. Graiff, G. Predieri, A. Tiripicchio, C. Vignali, J. Chem. Soc. Dalton Trans. (1999) 237–241;
(c) D. Cauzzi, C. Graiff, M. Lanfranchi, G. Predieri, A. Tiripicchio, J. Chem. Soc. Dalton Trans. (1995) 2321–2322;
(d) D. Cauzzi, C. Graiff, C. Massera, G. Predieri, A. Tiripicchio, D. Acquotti, J. Chem. Soc. Dalton Trans. (1999) 3515–3521;
(e) F.F. de Biani, C. Graiff, G. Opromolla, G. Predieri, A. Tiripicchio, P. Zanello, J. Organomet. Chem. 637–639 (2001) 586–594.
[14] D. Belletti, C. Graiff, C. Massera, A. Minarelli, G. Predieri, A. Tiripicchio, D. Acquotti, Inorg. Chem. 42 (2003) 8509–8518.
[15] H. Shen, S.G. Bott, M.G. Richmond, Inorg. Chim. Acta 241 (1996) 71–79.
[16] P. Braunstein, C. Graiff, C. Massera, G. Predieri, J. Rose, A. Tiripicchio, Inorg. Chem. 41 (2002) 1372–1382.
[17] (a) A.M.Z. Slawin, M.B. Smith, J.D. Woollins, J. Chem. Soc. Dalton Trans. (1997) 1877–1881;
(b) K. Raghuraman, S.S. Krishnamurthy, M. Nethaji, J. Organomet. Chem. 669 (2003) 79–86.
[18] T.S. Venkatakrishnan, M. Nethaji, S.S. Krishnamurthy, Curr. Sci. 85 (2003) 969–974.
[19] (a) K. Raghuraman, S.S. Krishnamurthy, M. Nethaji, J. Chem. Soc. Dalton Trans. (2002) 4289–4295;
(b) S.K. Mandal, G.A.N. Gowda, S.S. Krishnamurthy, M. Nethaji, Dalton Trans. (2003) 1016–1027;
(c) S.K. Mandal, G.A.N. Gowda, S.S. Krishnamurthy, C. Zheng, S. Li, N.S. Hosmane, J. Organomet. Chem. 676 (2003) 22–37;
(d) S.K. Mandal, G.A.N. Gowda, S.S. Krishnamurthy, T. Stey, D. Stalke, J. Organomet. Chem. 690 (2005) 742–750;
(e) M. Ganesan, S.S. Krishnamurthy, M. Nethaji, J. Organomet. Chem. 690 (2005) 1080–1091.
[20] (a) For reviews see: M.S. Balakrishna, V.S. Reddy, S.S. Krishnamurthy, J.F. Nixon, J.C.T.R.B.St. Laurent, Coord. Chem. Rev. 129 (1994) 1–90;
(b) M. Witt, H.W. Roesky, Chem. Rev. 94 (1994) 1163–1181;
(c) P. Bhattacharya, J.D. Woollins, Polyhedron 14 (1995) 3367–3388;
(d) K. Raghuraman, S.K. Mandal, T.S. Venkatakrishnan, S.S. Krishnamurthy, M. Nethaji, Proc. Indian Acad. Sci. (Chem. Sci.) 114 (2002) 233–246.
[21] (a) R.P.K. Babu, S.S. Krishnamurthy, M. Nethaji, Tetrahedron: Asymmetry 6 (1995) 427–438;
(b) R.J. Cross, T.H. Green, R.J. Keat, J. Chem. Soc. Dalton Trans. (1976) 1424–1428;
(c) M.S. Balakrishna, T.K. Prakasha, S.S. Krishnamurthy, U. Siriwardane, N.S. Hosmane, J. Organomet. Chem. 390 (1990) 203–216;
(d) M. Ganesan, Synthetic, Spectroscopic and Structural Investigations of Homo- and Heterodinuclear Transition Metal complexes of diphosphinoamine ligands, Ph.D. thesis, Indian Institute of Science, Bangalore, India, 1998.
[22] J.W. Faller, J. Lloret-Fillol, J. Parr, New J. Chem. 26 (2002) 883–888.
[23] E. Simon-Manso, M. Valderrama, P. Gantzel, C.P. Kubiak, J. Organomet. Chem. 651 (2002) 90–97.
[24] P.B. Hitchcock, J.F. Nixon, I. Silaghi-Dumitrescu, I. Haiduc, Inorg. Chim. Acta 96 (1985) 77–80.

[25] (a) Bruker SMART, V. 6.028, Bruker AXS Inc., Madison, Wisconsin, USA, 1998.;
(b) Bruker SAINT, V. 6.02, Bruker AXS Inc., Madison, Wisconsin, USA, 1998.;
(c) G.M. Sheldrick, SADABS, University of Göttingen, Germany, 1997;
(d) Bruker SHELXTL, NT V. 5.10, Bruker AXS Inc., Madison, Wisconsin, USA, 1998.
[26] L.J. Farrugia, J. Appl. Crystallogr. 32 (1999) 837–838.
[27] G.M. Sheldrick, SHELXL-97, Program for Refinement of Crystal Structures, University of Göttingen, Germany, 1997.
[28] (a) M.S. Balakrishna, M. Klein, S. Uhlenbrock, A.A. Pinkerton, R.G. Cavell, Inorg. Chem. 32 (1993) 5676–5681;
(b) R.P.K. Babu, K. Aparna, S.S. Krishnamurthy, M. Nethaji, Phosphorus, Sulfur, and Silicon 103 (1995) 39–53;
(c) P. Bhattacharya, A.M.Z. Slawin, D.J. Williams, J.D. Woollins, J. Chem. Soc. Dalton Trans. (1995) 3189–3194;
(d) P. Bhattacharya, J. Novosad, J. Phillips, A.M.Z. Slawin, D.J. Williams, J.D. Woollins, J. Chem. Soc. Dalton Trans. (1995) 1607–1613;
(e) D. Cupertino, R. Keyte, A.M.Z. Slawin, D.J. Williams, J.D. Woollins, Inorg. Chem. 35 (1996) 2695–2697.
[29] P. Diehl, H. Kellerhals, W. Neiderberger, J. Mag. Reson. 4 (1971) 352–357.
[30] (a) L. Marko, T. Madach, H. Vahrenkamp, J. Organomet. Chem. 190 (1980) C67–C70;
(b) R.D. Adams, J.E. Babin, M. Tasi, Organometallics 7 (1988) 219–227;
(c) R.D. Adams, I.T. Horvath, H.S. Kim, Organometallics 3 (1984) 548–552.